Acta Crystallographica Section D
Biological Crystallography
ISSN 0907-4449

Microscale vapour diffusion for protein crystallization

Justyna Korczyńska,[a] Ting-Chou Hu,[b] David K. Smith,[b] Joby Jenkins,[c] Rob Lewis,[c] Tom Edwards[c] and Andrzej M. Brzozowski[a]*

[a]Structural Biology Laboratory, Department of Chemistry, University of York, York YO10 5YW, England, [b]Department of Chemistry, University of York, York YO10 5DD, England, and [c]TTP LabTech Ltd, Melbourn Science Park, Melbourn, Royston SG8 6EE, England

Correspondence e-mail: marek@ysbl.york.ac.uk

Received 29 May 2007
Accepted 1 August 2007

The development of new crystallization platforms *via* the application of high-throughput technologies has delivered a plethora of crystallization plates suitable for robot-driven and manual setups. However, practically all these plates (except for microfluidic channel chips) are based on a very similar design and well (precipitant):drop (protein) volume ratios. A new type of crystallization plate (μplate) has therefore been developed and tested that still employs the classical vapour-diffusion technique but minimizes the precipitant well volume to 1.2 μl for a 150 nl protein drop setup. This enables a very significant saving on the total bulk of the crystallization screen, hence allowing the application of new, rare and expensive solutions in automated crystallization-screening procedures. Additionally, owing to the very low drop:well volume ratio, the new μplate can significantly accelerate the equilibrium time necessary for crystal nucleation and growth, in many cases shortening the high-throughput crystallization screening process to a few hours.

1. Introduction

Automation of the crystallization process has contributed significantly to the rapid progress of crystallography-based structural biology. For example, the 96-well plate format was seamlessly incorporated into robot-driven crystallization setups, enabling the high-throughput (HT) streamlining of this process. Current crystallization plates support the screening of thousands of conditions, automated optical evaluation of the results and frequently direct mounting and use of crystals for X-ray experiments without further optimization of the crystallization conditions (*e.g.* Berry *et al.*, 2006). It has also been shown that direct exposure of crystal-containing plates to X-rays from in-house sources is possible (*e.g.* PX Scanner by Oxford Diffraction; Yadav *et al.*, 2005; Eisenstein, 2007).

There are dozens of commercially available plates for everyday use in crystallization laboratories: *e.g.* CrystalQuick (standard/low profile) from Greiner; Crystal*EX*, COC, PZero and Crystal*EX* series from Corning; hanging drop from TPP and Intelli-plate from ArtRobbins. Recently, the MRC Laboratory of Molecular Biology (Cambridge, UK) incorporated a number of further improvements such as easy crystal retrieval through raised protein well surfaces and wide protein wells, easy viewing through new optically superior polymers, micronumbering of the wells and an extensive sealing surface. This fine-tuning of the design of the crystallization platform resulted in a new model of a very user-friendly plate (Innovaplate). The plethora of sitting/hanging-drop-oriented plates is further supplemented by many types of microbatch-devoted plates such as, for example, Greiner IMP@CT

(+/− reservoir) plate, Douglas Instruments Vapour Batch Plate, 72 Well Microbatch Plate and V Bottom 96-Well Microbatch Plate.

However, all currently available 96-well plates, with the exceptions of the microfluidic (Hansen *et al.*, 2002; Chen *et al.*, 2007) and counter-diffusion methods (Garcia-Ruíz *et al.*, 2002; Ng *et al.*, 2003), rigidly follow the SBS footprint for microplates (ANSI/SBS 1–2004; American National Standards Institute/Society for Biomolecular Sciences, Danbury, USA) and are variations of the same sitting- or hanging-drop principle and framework. Although rigorous maintenance of this format provides extremely useful compatibility of these plates with the 96-well format accepted by crystallization, plate-handling and imaging robots, this 'canonical' plate formatting also results in some experimental constraints. One of these limitations is the relatively conservative protein (∼25–150 nl): well (∼25–150 µl) ratio of solutions that can be applied during crystallization. Although this approach is supported overwhelmingly by statistics as a very efficient and most useful crystallization template, the designs of the plates, especially the relatively large size of the crystallization chambers, limit experiments with other hanging/sitting-drop setups. Most importantly, the relatively large consumption of precipitant per single reservoir well (∼50–100 µl) has practically prohibited the development and applications of new types of precipitants that could be obtained by more sophisticated, but expensive, organic syntheses. Therefore, the expansion of the chemical space in the protein crystallization is dramatically slow in comparison to other advances in this field.

To address these problems, we embarked on the development of a new type of crystallization plate that would (i) enable the testing and practical use of a new type of precipitant, (ii) minimize the consumption of these compounds, making the testing and application process economically viable, (iii) maintain satisfactory optical properties and (iv) facilitate straightforward crystal recovery and mounting. The design and execution of the new plate, referred here as to the µplate ('microplate'), was associated with our Wellcome Trust research projects on the chemical synthesis of new types of polymers and their applications in protein crystallization, which will be reported separately. As the approximate cost of synthesis of 1 g of the new substance in this project was in the range ∼£300–800, it was obvious that currently available crystallization plates would not even permit preliminary testing of these polymers. Indeed, small-scale preliminary experiments using available sitting-drop crystallization plates with a 150 nl protein drop and an ∼1–5 µl range of reservoir solution led to quick evaporation of the setup. Although it has been shown that the crystallant portion of the crystallization droplet does not have to be the same as the reservoir against which the droplet is equilibrated (Luft & DeTitta, 1995; Newman, 2005; Dunlop & Hazes, 2005), we found this approach unfeasible and too risky at this stage of the project as the crystallization properties of new polymers would be difficult to assess correctly. However, if the crystallization behaviour of the polymers can be established, the reservoir-saving alternative could be investigated further. Another alternative precipitant-saving approach by application of the widely tested and used microbatch method (*e.g.* Chayen, 1998) had also not been undertaken. The amphiphilic properties of the new polymers, allied to their high density, gel-like properties and intended use with membrane proteins, inclined us towards revisiting a sitting-drop-like setup, which could provide a more controllable assessment of the final chemical composition of the mother liquor. In brief, we believed that the sitting-drop-like crystallization platform should be a starting template for the assessment and preliminary applications of the new polymers. If they proved to be useful, they might be applicable to other suitable crystallization techniques.

The search for new precipitants required at the outset the formulation and availability of a new crystallization plate that would allow application of the precipitant solution within the range of a few microlitres equilibrated against approximately 150 nl protein solution.

We report in this paper the design and testing of a new type of crystallization plate, referred to as the µplate, that reduces precipitant consumption to as little as 1.2 µl. During the tests the µplate demonstrated some other beneficial characteristics such as very easy crystal retrieval and, most of all, a greatly accelerated rate of nucleation and crystal growth. The µplate can also simplify the distribution of all solutions required in the crystallization process as one robot can deliver the precipitant well solution (microlitre range) as well as the protein and precipitant components of the drops. We believe that the µplate can be considered to be a very useful supplement to the current armoury of existing plates and can at the same time open the way to new and exciting experimental possibilities.

2. Materials and methods

2.1. The development of the µplate

The main principles of the new µplate (*e.g.* low well-solution volume set against an ∼150 nl crystallization drop) and its prototype character resulted in a search for a new, thin and low-cost material that could be pressed into a suitable well profile, instead of the more costly and complex injection-moulding approach. Several materials have been tested: polypropylene (PP), polyethylene (PE), polyethylene terephtalate (PET) and polyethylene terephtalate glycol (PETG). Many plate-covering foils and lids with different surface and air-permeability properties were tested in order to secure the optimum sealing of the µplate (see below). The selection of a thin (250 µm) PETG film as the plate material required the design and testing of a solid support for the µplate for the crystallization-setup routine on the robot, as well as visual inspection and crystal harvesting. Therefore, a special µplate holder has been designed and tested (see below) to fit the spatial requirements of the Mosquito robot.

2.2. Test crystallizations

Test crystallizations were performed on two levels. Firstly, well characterized crystallization conditions for the test

proteins hen egg-white lysozyme (Sigma), *Trichoderma resei* xylanase (Hampton Research) and *Streptomyces rubiginosus* glucose isomerase (GI; Hampton Research) were explored. Secondly, when the spatial parameters of the µplate had been optimized it was made available to the research staff of the YSBL (York Structural Biology Laboratory) for applications and tests on regular crystallization projects.

The previously reported test crystallization conditions for lysozyme, xylanase and GI were first refined prior to their application on the µplate. In this process, the hanging-drop technique was used on standard 24-well Linbro tissue plates with 1 ml well solution and 1 µl protein + 1 µl well crystallization drops, with variations of the initial test conditions. The most reproducible conditions with a regular maximum yield of crystals were found to be as follows: lysozyme, protein concentration (cp) = 30 mg ml^{-1} (protein in 50 m*M* sodium acetate buffer pH 5.0), 0.1 *M* sodium acetate buffer pH 4.5, 1.0 *M* NaCl; xylanase, cp = 35 mg ml^{-1} in 50 m*M* Tris–HCl pH 7.5; condition *A*, 0.1 *M* Tris–HCl pH 8.5, 0.2 *M* LiCl, 20%(*w*/*v*) PEG 4000; condition *B*, 0.1 *M* MES pH 6.5, 0.2 *M* LiCl, 20%(*w*/*v*) PEG 4000; GI, cp = 38 mg ml^{-1} in 50 m*M* Tris–HCl pH 7.5; condition *A*, 0.1 *M* Tris–HCl pH 7.0, 0.2 *M* $MgCl_2$, 20%(*v*/*v*) PEG 400; condition *B*, 0.1 *M* Tris–HCl pH 7.0, 0.2 *M* $MgCl_2$, 23%(*v*/*v*) MPD. Subsequently, large stock solutions of these conditions were made and applied in tests of the µplate. All crystallizations were carried out at room temperature (292 ± 0.5 K).

To find the optimum ratio of crystallization solutions, the drop size was set at a standard 150 nl (precipitant) + 150 nl (protein) size and the volume of the reservoir solution was varied from 0.3 to 3 µl. The final optimal crystallization setup of the µplate consisted of a 150 nl + 150 nl drop equilibrated against 1.2 or 2.4 µl well solution. Three different covers were tested: ThermalSeal RT (Web Scientific Ltd), CrystalClene Sheets (Molecular Dimensions Ltd) and Crystal Clear Sealing Tape (Hampton Research).

For assessment of the performance of the µplate, the same crystallization conditions were also applied on the commonly used Greiner CrystalQuick low-profile plate and on the Nunc-Immuno 96 MicroWell hanging-drop plate with ThermalSeal RT (Web Scientific Ltd) cover. The standard 150 nl protein + 150 nl precipitant, 100 µl well solution setup was used for both type of plates and techniques.

In each case, multiple crystallizations were performed in order to find the optimum setups. Table 1 lists the average results for the three optimized typical repeats.

All crystallization plates (except the initial 24-well hanging-drop optimization trays) were set up by a Mosquito robot (TTP Labtech), including the transfer of the precipitant to the µplate well compartment. For this particular reason, screen solutions were distributed and stored in more shallow Nunc-Immuno 96 MicroWell Plates (Nunc) as the commonly used MegaBlock 96 Well 2.2 ml PP (Sarstedt) storage blocks were too deep to be penetrated effectively by the needles of this robot.

Images of the crystallization setups (Fig. 3) were taken on a Leica MZ125 microscope equipped with a JVC 3-CCD colour

Table 1
Average crystallization results of a typical three repetitions of the test conditions on µplate, Greiner sitting-drop plate and hanging-drop plate.

Average numbers of drops from a typical three repetitions of lysozyme, glucose isomerase and xylanase crystallization on the µplate, Greiner-sitting drop (Greiner CrystalQuick low-profile plate) and hanging drop (Nunc-Immuno 96 MicroWell hanging-drop) plates. Time corresponds to the intervals between manual inspections of the plates (each protein had its specific growth time scale).

(*a*) Lysozyme.

Time (h)	µplate	Greiner sitting drop	Hanging drop
0.25	31	0	0
0.5	41	0	12
1	52	19	75
2.5	60	22	94
3.5	68	35	94
7.5	72	37	94
12	72	41	94
24	81	45	94

(*b*) Glucose isomerase.

	µplate		Greiner sitting drop		Hanging drop	
Time (h)	Condition *A*	Condition *B*	Condition *A*	Condition *B*	Condition *A*	Condition *B*
1	96	31	96	18	88	26
3	96	36	96	21	88	38
6	96	36	96	21	88	38
24	96	44	96	21	88	38

(*c*) Xylanase.

Time (h)	µplate	Greiner sitting drop	Hanging drop
1	50	0	75
4	80	31	86
24	90	41	96

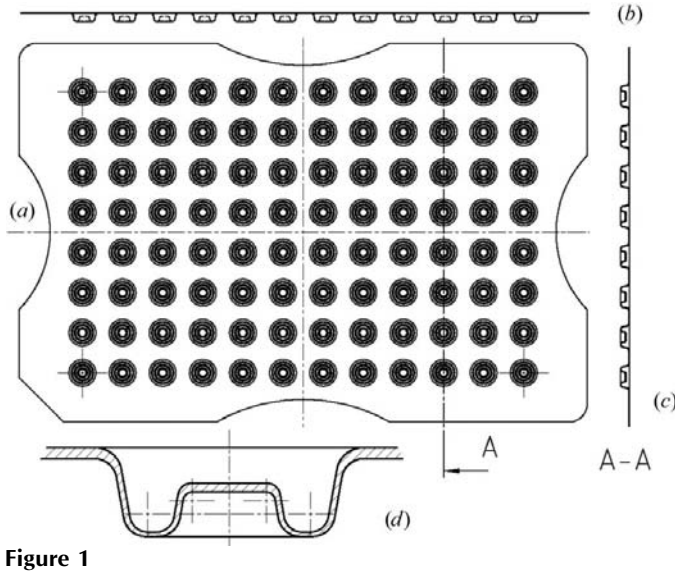

Figure 1
Scheme of the µplate. (*a*) Overall top view of the µplate; (*b*) and (*c*) side projections; (*d*) close-up of one crystallization chamber. The overall dimensions of the µplate are 127.5 × 85 mm; the thickness of the plate (including well) is 2 mm; the crystallization chamber has a diameter of 4 mm and a depth of 2 mm and the ledge for the crystallization drop has diameter of 1.8 mm. The overall design of the µplate follows the SBS footprint.

video camera (Model KY-F55B) and *AcQuis Bio* v.3.1 digital imaging software (Syncroscopy).

3. Results and discussion

3.1. µplate design and testing

Several designs of vapour-diffusion microplates were considered. The main objective was the radical minimization of the volume of the precipitant necessary for the crystallization whilst simultaneously maintaining all of the benefits of the classical vapour-diffusion technique: *i.e.* simplicity of setup, easy optical evaluation of the drops/crystal growth and straightforward retrieval of the crystals. The cost of synthesis of the new polymers/precipitants that we wanted to apply in protein crystallization constrained the volume of the well to be well below ∼10 µl if their everyday use were to be economically viable. Several preliminary concepts for the new crystallization-plate analogue were considered and small circular wells with a centrally based protein-drop platform were selected (see Figs. 1 and 2) for further experiments. To minimize the cost of testing trials and the overall cost of the trays, the pressing/mould technology rather than the injection approach was preferred for the plate-production process. This led to the formation of the 96-well µplate with a classical SBS footprint but with a very thin (250 µm) PETG foil plate body and a very low overall height, including the crystallization chamber, of 2 mm. The principal layout of the µplate design is a centrally located platform or ledge for deposition of the protein and precipitant drops, which is surrounded by a circular depression channel that can accommodate up to 10 µl reservoir solution depending on properties such as viscosity or detergent content.

The optimization of the volume of the crystallization chamber was crucial for the final success of this design. If the head volume over the precipitant solution was too large this resulted in the accelerated evaporation of both precipitant and the drop containing protein, while a very small chamber caused mixing of both solutions and the bridging of the protein drop with the low-hanging cover/seal. The optimum volume of the whole chamber was found to be around 35 mm^3. The elevated platform or ledge for the deposition of the protein and the precipitant nano-drops could accommodate a volume of up to 500 nl.

Setting the crystallization drop size at typically 150 nl + 150 nl and varying the reservoir solution volume from 0.3 to 2 µl, the minimum usable volume of the precipitant ('well') solution was found to be 1.2 µl, resulting in a very low 1:8 protein drop:well ratio (see Fig. 3). Any lower well volume resulted in an accelerated evaporation of the crystallization drops, despite the appearance of some crystals. This 1:8 (drop:well) ratio is well below the corresponding current lowest (∼1:333) ratio that can be achieved in a typical crystallization plate such as the MRC LMB (Innovaplate) plate (assuming a standard 150 nl + 150 nl setup against 50 µl well solution). Consequently, this extremely low drop:reservoir ratio allowed realistic applications and testing of the new precipitants. However, the low µplate reservoir volume may also have a positive impact on rudimentary systematic crystallization screening procedures as it can also be used with all available commercial/in-house screens, leading to unprecedented savings on the cost of solutions and substantial improvement of the economy of the crystallization-screening process.

The additional advantage that results from the 1.2 µl (minimum) well volume of the µplate is the possibility of employing the same crystallization robot (Mosquito in this case) not only for setting up the crystallization drops but also for distribution of the reservoir solution. As the volume of 1.2 µl is within the range of the positive dispensing capacity of Mosquito needles, a new software protocol was written for this robot that allowed its use for the complete setup (drops + well reservoir distribution) of the whole plate. Therefore, automated pipette or well-filling robots may not be necessary for the µplate crystallization setup. However, this approach requires replacement of the standard deep-well screen storage

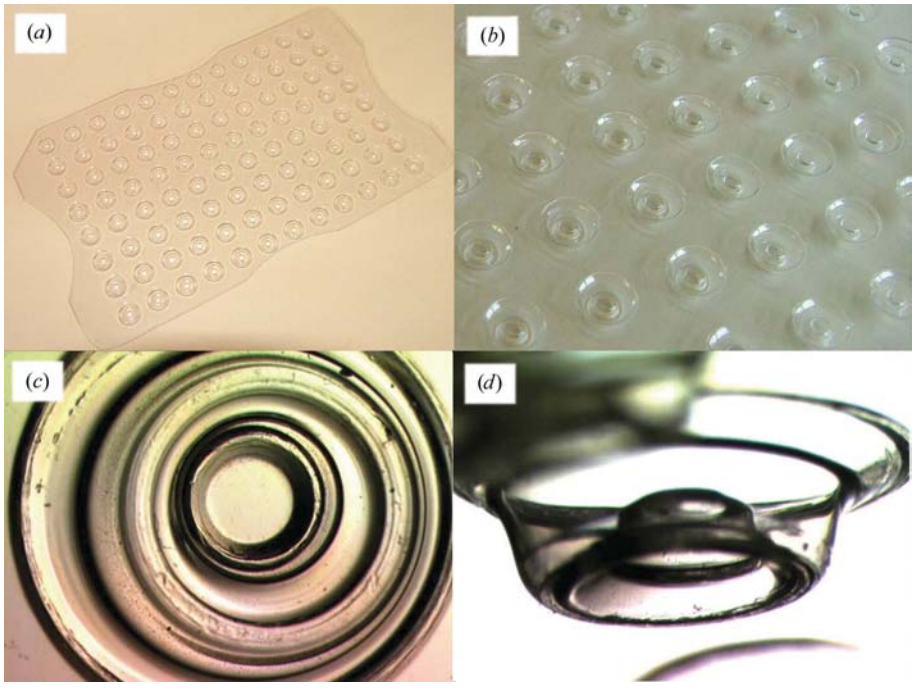

Figure 2
Some snapshots of the µplate. (*a*) Overall view of 96-well µplate compatible with the SBS format; (*b*) close-up of the microcrystallization chambers; (*c*) top view of a single crystallization chamber with central ledge for positioning of the crystallization drop and surrounding circular channel for dispensing the precipitant solution; (*d*) sideways view of a single crystallization chamber.

blocks by lower (and smaller volume) solution carriers such as Nunc-Immuno 96 MicroWell Plates (in the case where the Mosquito robot is being used).

3.2. Crystallization validation of the µplate

3.2.1. The seal. The very small volume of the whole setup required very effective control of the evaporation problem. Three different covers/seals were tried in order to evaluate the best sealing and evaporation-protection properties. The ThermalSeal RT cover was found to be best for this particular application, delaying the first signs of drying for at least 72 h. Crystal Clear Sealing Tape also gave reasonable protection, but the short distance between the µplate surface and the top of the drop, combined with the relative flexibility of this tape and the slight pressure required during its application, resulted in occasional contact of the seal with the crystallization drop. CrystalClene Sheets also showed very good sealing properties, but their relatively high price was in contrast with the overall low-cost principle of our approach and they were thus not selected for further trials.

3.2.2. The µplate holder. The thinness of the µplate improved the optical evaluation of the crystallization results. The manual handing of the µplate under the microscope is

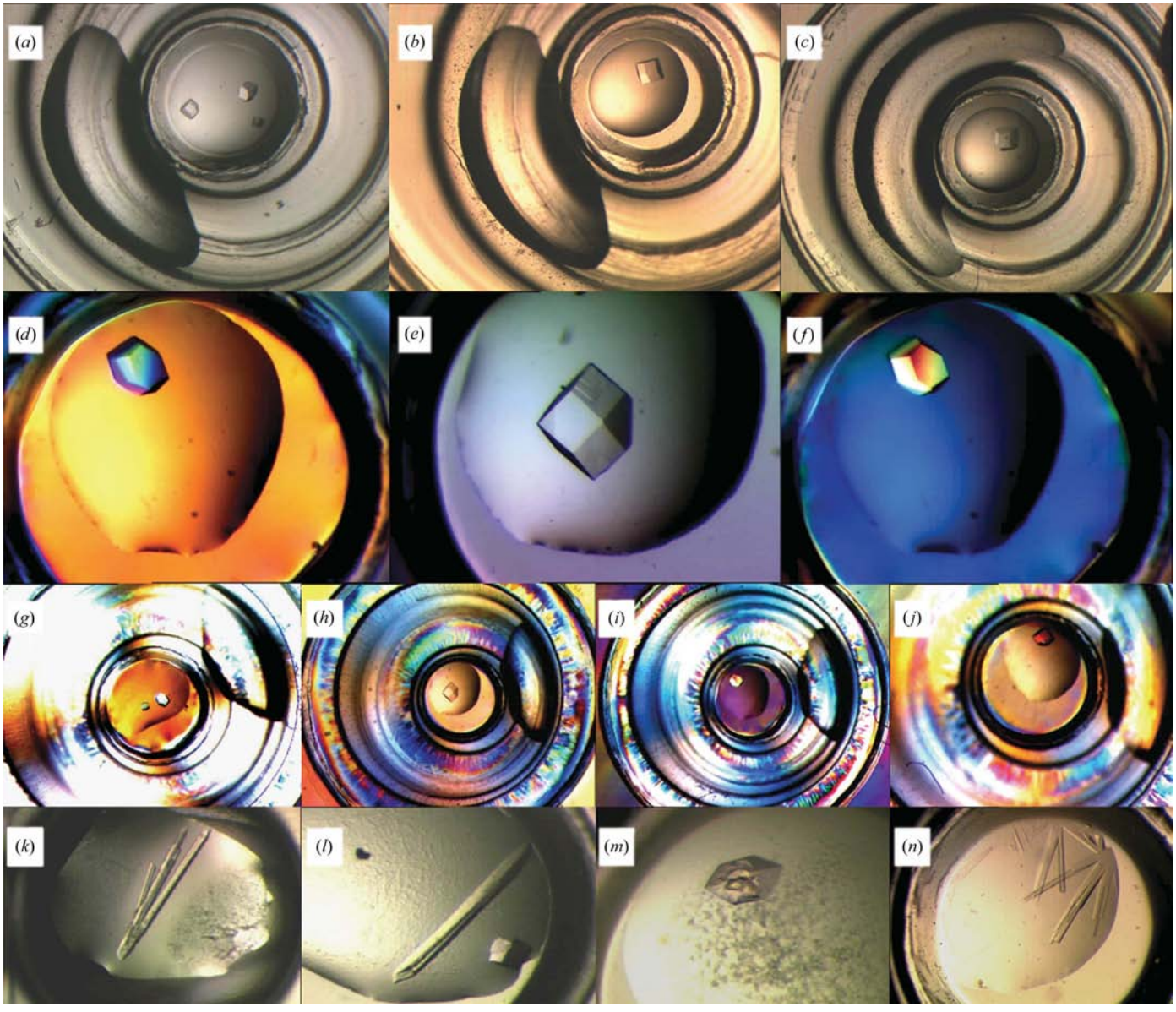

Figure 3
Microscope camera snapshots of some typical µplate crystallization setups. (*a*) and (*b*), lysozyme setups with the 1.2 µl precipitant drop in the circular channel and a 150 + 150 nl protein/precipitant drop on the central ledge. (*c*) Glucose isomerase setup, volumes as in (*a*) and (*b*). (*d*)–(*f*) Close-ups of lysozyme setups with different orientations of microscope polarizers. (*g*)–(*j*) Top view of typical µplate crystallization setups with different orientations of the microscope analyser/polariser: the optical properties of the crystallization drop platform are undisturbed in this process and allow easy identification of the crystallization results in all conditions. (*k*)–(*m*) 'Real project' AcfC protein crystals that appeared within 6 h after the setup and were used directly for SAD X-ray data collection (at 1.4 Å resolution) and structure solution. (*n*) A different (to that in *c*) crystal form of glucose isomerase.

unhindered by the relatively flexible mechanical properties of the plate. However, if preferred, the special holder that has to be used during the crystallization setup can also be applied during visual inspection of the drops and crystal harvesting (Fig. 4).

The current version of the magnetized two-piece metal holder (similar to the metal base used by the Mosquito robot as a support for the hanging-drop crystallization plate seal) consists of a base support structure and a magnetic top that clamps and presses the μplate firmly to the base. The holder has been developed with the dimensions of the typical SBS footprint, with 96 through holes corresponding to the positions of individual crystallization chambers (Fig. 4). The holder allows easy setup of the drops on the Mosquito robot (and presumably on any other SBS-compatible robots) as well as assisting in visual inspection of the μplate on a microscope (in the manual or automated mode). It may also provide an additional support for easy crystal harvesting. However, its use outside the actual crystallization setup may not be necessary and is user-dependent. Crystal retrieval is rather straightforward, as the small dimensions of the crystallization chamber and close-to-surface position of the ledge allow a very wide, comfortable angle for crystal fishing.

3.2.3. Test crystallizations. Three standard test proteins, lysozyme, glucose isomerase (GI) and xylanase, were employed in the calibration and validation of the μplate. The crystallization conditions for these proteins were optimized prior to plate tests in order to assure their maximum efficiency and reproducibility (the final conditions are given in §2). One crystallization condition was applied for lysozyme crystallization and two for GI and xylanase crystallization. However, after preliminary trials condition *B* for xylanase [0.1 *M* Tris–HCl pH 7.0, 0.2 *M* $MgCl_2$, 23%(*v*/*v*) MPD] was found to not be as reliable or reproducible as condition *A* and hence was not used any further in the evaluation of the μplate. Some typical results of the test crystallizations are summarized in Table 1. It must be stressed that the crystallization data presented here cannot serve as a full and proper evaluation of the trays used in these trials. This would require a separate much more statistically stringent approach. The main objective of our efforts here was a simple comparison of the usability of the new μplate against the most commonly used trays and test proteins.

It is clear that the 1:8 drop:well volume ratio achieved in the μplate footprint can serve as a new reliable solution-equilibrium system for protein crystallization. Test crystals were achieved in the μplate with the same or better frequency than in Greiner CrystalQuick low-profile and hanging-drop Nunc-Immuno 96 MicroWell plates. It is interesting that the μplate crystal-growth rate was more comparable with the hanging-drop setup than with the sitting-drop technique on the Greiner plate. However, a reliable assessment of this trend would require further experiments.

One of the other interesting features of the μplate emerging from these tests is an extremely fast rate of appearance of crystals. Usually, the first crystals of test proteins were observed in the first few minutes after setup. It is likely that the proximity of the sitting drop and the well solution, which are enclosed in a very small chamber, results in accelerated mass transfer, drop evaporation and the establishment of a crystal-growth-inducing well–drop equilibrium. As our aims here were purely practical, *i.e.* the construction of a plate that worked well with the microwell precipitant volume, we did not intend to further pursue this type of investigation. However, our preliminary observations here are in agreement with theoretical (*e.g.* Diller & Hol, 1999) and experimental data (DeTitta & Luft, 1995; Luft & DeTitta, 1995; Luft *et al.*, 1996; Santarsiero *et al.*, 2002) showing that the most likely equilibrium rate-limiting step during vapour-diffusion-based crystallization is the diffusion of water from the drop to the reservoir; it is likely that the transit of water through the volume of the crystallization chamber in the μplate would be the fastest of all currently used crystallization plates. Although the fast equilibrium time is not necessarily an immediate advantage in the crystallization process and can lead, for example, to amorphous precipitation of protein or showers of microcrystals (García-Ruiz, 2003), these unwanted trends were not observed in the μplate on a level that would warrant concern.

In general, taking into account the rate of crystal appearance, the evolution of drop content and the first signs of some evaporation/drying out after few (∼4/5) days, we consider the μplate to

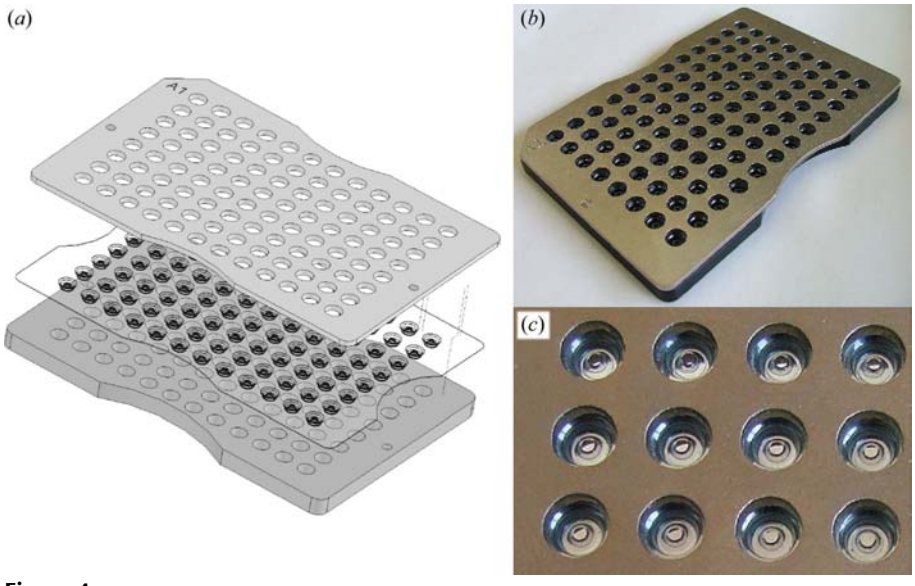

Figure 4
The μplate holder. (*a*) Schematic of the overall principle of the holder: the μplate is inserted between the base and the top, which are magnetized. (*b*) View of the holder with the μplate; this setup fits the 96-well SBS footprint. (*c*) Close-up of the holder with the μplate: the drill-through base of the holder enables easy evaluation of the crystallizations under a microscope and manipulation of the crystals if necessary.

be a useful platform for rapid (3–5 d maximum) crystallization experiments. The μplate crystallization rate suggests that practically 100% of the final results of the crystallizations [including the maturation and growth of the rapidly (minutes to hours) emerging small crystals] were usually achieved within 72 h of setup. Further monitoring of these crystallizations did not reveal any new features or new crystals.

The fast crystal growth and quite possibly unique equilibrium phenomena occurring on the μplate may have implications for its wider applications. It may not only be useful for the screening of solutions of limited availability (or for economy-based reasons), but typical standard screens can also be revisited on the μplate if they have failed on currently used crystallization plates. The different mass-transfer phenomena that occur in the μplate chamber may lead to nucleation and crystal growth under conditions that were unsuccessful on other crystallization platforms. Moreover, the design of the μplate allows multiple distributions of drops of precipitants into the circular channel surrounding the crystallization platform. For example, two 1.2 μl drops were dispensed to slow the vapour-diffusion equilibrium when necessary.

In addition to tests using standard proteins, the μplate was also examined in regular ongoing research projects within the YSBL. Although the results cannot be fully reported here, several crystal forms of one of the proteins (AcfC) were obtained in the μplate in a short crystallization time (∼6 h) using commercial screens (Fig. 3, courtesy of Axel Müller). The crystals were easily picked up into the loops and cryoprotected and a SAD X-ray data set was collected at the ESRF. This crystal structure was subsequently solved and refined at 1.4 Å resolution and will be published elsewhere (Axel Müller, personal communication).

4. Conclusions

In summary, we have designed, tested and validated a new crystallization plate that has quite different properties from other currently used crystallization platforms. The μplate, which works on the principle of microvolume vapour diffusion, provides several new interesting characteristics. It allows use of rare and expensive precipitants, reduces the time necessary for crystal nucleation/growth and facilitates easy harvesting of the crystals. The low-cost μplate design, fast crystal growth and 40–80-fold minimization of screen consumption make it a new and interesting crystallization-platform alternative for everyday use in structural biology laboratories. In addition, with the advent of *in situ* in-house X-ray diffraction crystal evaluation (*e.g.* PX Scanner, Oxford Diffraction), the ultrathin μplate material and construction may assure the optimum environment for this type of application.

We are grateful to Axel Müller, Elena Blagova and Mark Fogg of the YSBL for testing of the μplate on their ongoing projects. The YSBL part of this research was supported by Wellcome Trust Grant 072827/Z/03/Z, on which JK and T-CH were also employed.

References

Berry, I. M. *et al.* (2006). *Acta Cryst.* D**62**, 1137–1149.
Chayen, N. E. (1998). *Acta Cryst.* D**54**, 8–15.
Chen, D. L. L., Li, L., Reyes, S., Adamson, D. N. & Ismagilov, R. F. (2007). *Langmuir*, **23**, 2255–2260.
DeTitta, G. T. & Luft, J. R. (1995). *Acta Cryst.* D**51**, 786–791.
Diller, D. J. & Hol, W. G. J. (1999). *Acta Cryst.* D**55**, 656–663.
Dunlop, K. V. & Hazes, B. (2005). *Acta Cryst.* D**61**, 1041–1048.
Eisenstein, M. (2007). *Nature Methods*, **4**, 95–102.
García-Ruiz, J. M. (2003). *J. Struct. Biol.* **142**, 22–31.
Garcia-Ruíz, J. M., Gonzalez-Ramirez, L. A., Gavira, J. A. & Otálora, F. (2002). *Acta Cryst.* D**58**, 1638–1642.
Hansen, C. L., Skorodalakes, E., Berger, J. M. & Quake, S. R. (2002). *Proc. Natl Acad. Sci. USA*, **99**, 16531–16536.
Luft, J. R., Albright, D. T., Baird, J. K. & DeTitta, G. T. (1996). *Acta Cryst.* D**52**, 1098–1106.
Luft, J. R. & DeTitta, G. T. (1995). *Acta Cryst.* D**51**, 780–785.
Newman, J. (2005). *Acta Cryst.* D**61**, 490–493.
Ng, J. D., Gavira, J. A. & García-Ruiz, J. M. (2003). *J. Struct. Biol.* **142**, 218–231.
Santarsiero, B. D., Yegian, D. T., Lee, C. C., Spraggon, G., Gu, J., Scheibe, D., Uber, D. C., Cornell, E. W., Nordmeyer, R. A., Kolbe, W. F., Jin, J., Jones, A. L., Jaklevic, J. M., Schultz, P. G. & Stevens, R. C. (2002). *J. Appl. Cryst.* **35**, 278–281.
Yadav, M. K., Gerdts, C. J., Sanishvili, R., Smith, W. W., Roach, L. S., Ismagilov, R. F., Kuhn, P. & Stevens, R. C. (2005). *J. Appl. Cryst.* **38**, 900–905.